Electronic Supplementary Information

Quantitative temperature mapping within operating catalyst by spatially resolved ^{27}Al NMR

Anna A. Lysova,[a,b] Alexander V. Kulikov,[c] Valentin N. Parmon, [c] Renad Z. Sagdeev,[a] Igor V. Koptyug*[a,b]

[a]*International Tomography Center, SB RAS, Institutskaya St. 3A, Novosibirsk 630090, Russia*

[b]*Novosibirsk State University, Pirogova St. 2, Novosibirsk 630090, Russia*

[c]*Boreskov Institute of Catalysis, SB RAS, Acad. Lavrentiev Pr. 5, Novosibirsk 630090, Russia*

Table of Contents

1. Description of the reactor for spatially resolved NMR thermometry experiments.

The reactor (Fig. S1) comprised a glass tube 1 with an inner diameter of 10 mm in which a cylindrical 4% Pt/γ-Al_2O_3 catalyst pellet of 4.2 mm in diameter and ca. 10 mm long (A) was placed. This pellet was either glued to the reactor wall from the inside to cause the temperature non-uniformity within the pellet during the reaction (NMR imaging experiments), or placed in the center of the tube on a glass capillary or a

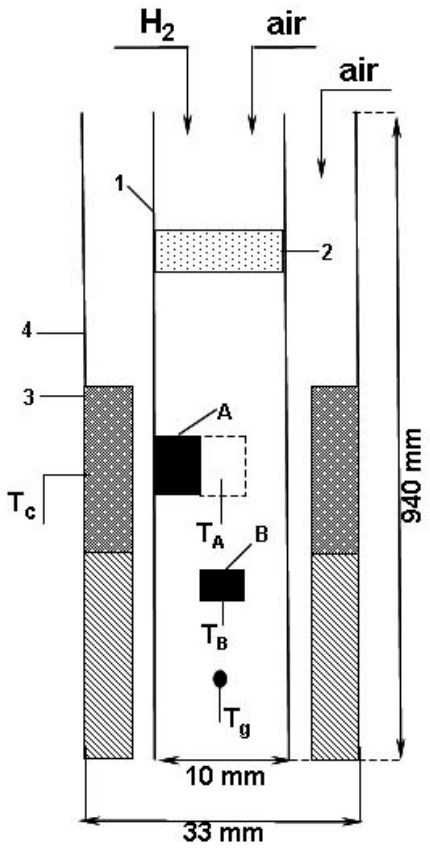

Figure S1. Schematic representation of the model catalytic reactor used for catalytic gas phase hydrogen oxidation inside the vertical bore NMR imaging instrument. A - main catalyst pellet (solid rectangle shows pellet position in the MRI thermometry experiments; dashed rectangle shows its position in the calibration experiments); B - reference catalyst pellet; 1 – glass reactor tube; 2 – stainless steel mesh used as a flame arrestor; 3 – radiofrequency coil; 4 – polypropylene tube; T_A and T_B – thermocouples measuring the temperatures of pellets A and B, respectively; T_c – thermocouple that monitors the temperature of the radiofrequency coil; T_g – thermocouple that measures temperature of the gas stream. A stream of air outside the reactor tube protects the instrument form overheating.

thermocouple to ensure the uniform temperature distribution (calibration experiments). A similar catalyst pellet (B, same composition but smaller in size) was placed ca. 8 mm below the main pellet. It was used to estimate the temperature of the main pellet A in the NMR imaging experiments when it was not possible to measure temperature with a thermocouple because of the possible distortion of the NMR signal inside the pellet around the implanted thermocouple.[S1] The gaseous mixture of hydrogen and air was supplied into the reactor tube. The rate of hydrogen supply was varied during the experiment in the range 0.5 – 3.0 cm^3/s, whereas the rate of air supply was constant and equal to 180 cm^3/s. A thermocouple located below the reference catalyst pellet B was used to measure the temperature of the flowing gas (T_g). Another thermocouple (T_c) was used to monitor the temperature of the rf coil 3 during the experiment to avoid

overheating of the gradient coils of the NMR imaging instrument. The glass reactor tube was placed inside a polypropylene tube 33 mm in diameter (4). Air was supplied in the gap between the glass reactor tube and the polypropylene tube at a flow rate selected in such a way that the temperature of the rf coil did not exceed 33 °C at the highest hydrogen flow rate used. A crumpled piece of stainless steel mesh (2) used as a flame arrestor was placed in the reactor tube 760 mm upstream of the main pellet in order to avoid an accidental flame propagation.

2. ^{27}Al NMR imaging and thermometry experiments.

The NMR imaging experiments were performed on a Bruker Avance DRX 300 NMR spectrometer equipped with imaging accessories. The ^{27}Al NMR signal was detected at the frequency of 78.172 MHz. The 2D imaging of γ-Al_2O_3 was performed using a two-pulse spin-echo pulse sequence[S2,S3] (α– τ – 2α– τ – echo) with τ ca. 250 μs. The two pulses had the same amplitude and were 8 and 16 μs long, respectively, corresponding to the nominal flip angle α = 30°. The 2D images were acquired in the plane transverse to the vertical axis of the reactor and the catalyst pellet. The two spatial coordinates (*x* and *y*, transverse to the vertical axis of pellet A) were phase encoded by an independent stepwise variation of two pulsed gradients G_X and G_Y (16 steps in the range -100 to 100 G/cm). The gradient pulses were 120 μs long and were applied during the first interval τ. Before Fourier transformation, the 16×16 data matrix was zero-filled to 128×128 data points. Additionally, sine filter was applied in both spatial dimensions (for the reconstruction of temperature maps only). A field of view FOV_{XY} = (6.1×6.1) mm^2 was imaged with a true spatial resolution of 0.384×0.384 mm^2 and a digital resolution of

0.04×0.04 mm^2 obtained after zero-filling. A larger FOV was used to obtain the image shown in Fig. 1b of the main text to visualize both the pellet and the glass reactor tube. However, the image shows that the ^{27}Al NMR signal intensity of the glass tube is much lower than that of the catalyst pellet. Therefore, in the spatially resolved thermometry experiments it was ignored and the field of view was reduced to image the pellet only. No slice selection was used in these experiments. Each pixel in the image thus corresponds to a voxel size of 0.384 mm × 0.384 mm × 10 mm = 1.47 microliters (1.47 mm^3). The pulse sequence repetition time was 300 ms. As a result, little signal suppression (T_1-weighting of the image) was expected at room temperature as the spin lattice relaxation time T_1 at this temperature was estimated as ca. 110 ms. As the T_1 time of the ^{27}Al NMR signal of γ-Al_2O_3 decreases with temperature,[S2] no signal suppression due to fast repetition of the pulse sequence is to be expected at elevated temperatures. To improve image detection sensitivity, signal averaging with 16 accumulations was used, resulting in the acquisition time of each 2D image of 20 min 56 s.

Fig. S2 compares the images acquired for the pellet positioned at the reactor wall to the images of the same pellet placed on the axis of the reactor. This comparison clearly demonstrates that under reactive conditions the ^{27}Al NMR signal intensity is much more uniform within the pellet when it is located at the axis and the gas flow pattern around the pellet is essentially axially symmetric, which is not the case when the pellet is displaced to the reactor wall to intentionally make the geometry of flow around the pellet non-uniform. As the ^{27}Al NMR signal intensity directly reflects the temperature of the catalyst, this comparison unambiguously verifies the fact the heterogeneous distribution

of temperature within the pellet (Fig. 3 of the paper) is caused by the asymmetric positioning of the pellet within the model reactor.

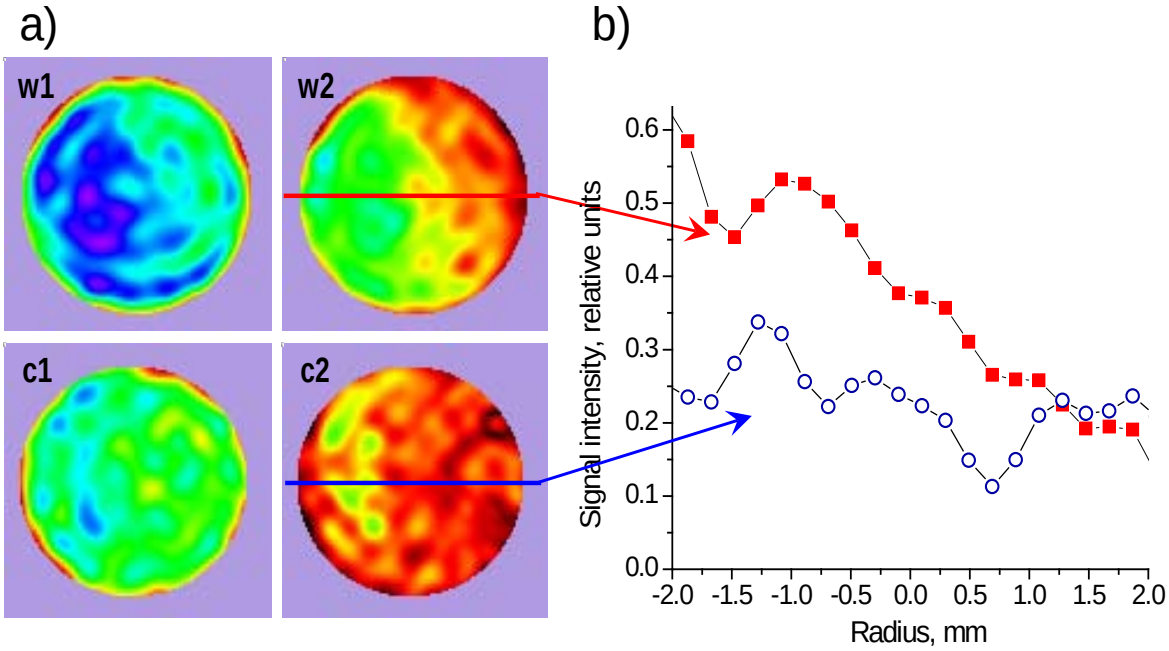

Figure S2. a) 2D ^{27}Al NMR images of the catalyst pellet detected during the catalytic oxidation of H_2. Images w1 and w2 were detected for the pellet positioned at the wall of the reactor tube, with H_2 flow rates of 0.75 (w1) and 2.49 (w2) cm^3/s. Images c1 and c2 were detected for the same pellet positioned axisymmetrically at the center of the reactor tube, with H_2 flow rates of 0.52 (c1) and 2.74 (c2) cm^3/s. b) Central 1D cross-sections of images w2 (red squares) and c2 (blue circles).

3. Constructing the calibration curve.

The following procedure was used to construct the calibration curve that relates the ^{27}Al NMR signal intensity of the solid phase (γ-Al_2O_3) to its temperature. The same catalyst pellet used in the NMR imaging experiment described above (pellet A) was placed in the center of the reactor (Fig. S1, dashed rectangle). It was supported by a thermocouple inserted in a small hole made through the lower flat surface of the pellet. The dependence of the temperature of pellet A on the temperature of pellet B was

measured in this experiment in the regimes with the same hydrogen and air flow rates as in the NMR imaging experiment. This $T_A(T_B)$ dependence was found to be linear. It allows one to evaluate the temperature of pellet A if the temperature of pellet B is known. In another experiment, the same catalyst pellet A placed in the center of the reactor was supported with a glass capillary instead of a thermocouple. This arrangement was used to perform the NMR imaging experiments and to detect the 2D ^{27}Al NMR images of this pellet in the regimes with various hydrogen flow rates (same as above). The 2D ^{27}Al NMR images detected in this experiment showed a more or less uniform NMR signal intensity distribution in the image plane. The ^{27}Al NMR signal was integrated over the entire image of the catalyst pellet and divided by the ^{27}Al NMR signal integrated over the pellet image acquired at room temperature. From the temperature of pellet B measured simultaneously with image acquisition, the temperature of pellet A was calculated using the $T_A(T_B)$ dependence described above. As a result, the dependence of the pellet temperature on the inverse normalized NMR signal intensity was constructed (Fig. S3).

The data points above room temperature can be fitted quite

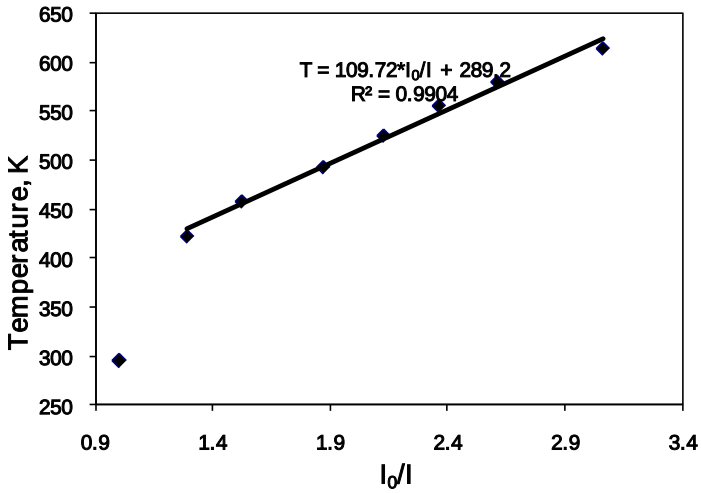

Figure S3. The calibration curve that relates the catalyst pellet temperature and the inverse normalized ^{27}Al NMR signal intensity averaged over the respective calibration image. The data points acquired at elevated temperatures were fitted with a straight line which is shown in the graph along with the fitting parameters.

well with a straight line. According to the Curie's law, this line, when extrapolated, should pass through the origin of the coordinate plane. However, this is not the case here. The likely reason is that the spin-spin relaxation time T_2 of ^{27}Al decreases with increasing temperature. As a result, the NMR signal intensity decreases with temperature faster than would be expected from the Curie's law alone. At room temperature, the measured T_2 relaxation time for the catalyst pellet was ca. 2 ms. With the echo time of 0.534 ms used in the NMR imaging experiments, this leads to very little T_2 weighting of the detected signal, and as a result this data point does not follow the trend of the rest of the data. In addition, some degree of T_1 weighting for the room-temperature data point makes this point fall further away from the trend defined by the rest of the data points that experience no T_1-weighting.

Finally, we note that the spatially resolved thermometry technique presented here is potentially applicable to other oxide supports that contain substantial concentrations of ^{27}Al nuclei, but the sensitivity of such measurement will depend on the Al content of the material. However, this approach may not work for Al-containing zeolites as ^{27}Al NMR signal intensity can drastically change with the changes in coordination of an Al atom in a solid material. Additional experiments will be needed to address this issue.

Additional references.

[S1] I.V. Koptyug, A.V. Kulikov, A.A. Lysova, V.A. Kirillov, V.N. Parmon, R.Z. Sagdeev. NMR imaging of the distribution of the liquid phase in a catalyst pellet during alpha-methylstyrene evaporation accompanied by its vapor-phase hydrogenation, *J. Amer. Chem. Soc.* **2002**, *124*, 9684-9685.

[S2] I.V. Koptyug, D.R. Sagdeev, E. Gerkema, H. Van As, R.Z. Sagdeev. Solid-state ^{27}Al MRI and NMR thermometry for catalytic applications with conventional (liquids) MRI instrumentation and techniques, *J. Magn. Reson.* **2005**, *175*, 21-29.

[S3] I.V. Koptyug, A.A. Lysova. Multinuclear NMR imaging of rigid solids with an Avance DRX-300, *Bruker Spin Repor*t **2006**, *157-158*, 22-25.